Articles

Rh(III) Porphyrins as Building Blocks for Porphyrin Coordination Arrays: From Dimers to Heterometallic Undecamers

James E. Redman,[†] Neil Feeder,[†] Simon J. Teat,[‡] and Jeremy K. M. Sanders*[,†]

Cambridge Centre for Molecular Recognition, University Chemical Laboratory, University of Cambridge, Lensfield Road, Cambridge, CB2 1EW, UK, and CLRC Daresbury Laboratory, Daresbury, Warrington, WA4 4AD, UK

Received September 13, 2000

The coordination chemistry of a Rh(III) porphyrin building block was investigated with a view to the construction of heterometallic arrays of porphyrins. The Rh(III) porphyrin was found to coordinate methanol in the solid state and weakly in $CDCl_3$ solution. Crystallization afforded five coordinate π stacked Rh(III) porphyrins. The distribution of products from reaction of Rh(III) porphyrin with DABCO, 4,4′-bipyridine, and 4,4′-bipyrimidine could be displaced toward dimeric species by silica gel column chromatography or recrystallization which served to remove excess ligand. Weak coordination to nitriles was observed, although it was sufficiently strong to organize a dimeric complex of 5,5′-dicyano-2,2′-bipyridine in the solid state. Complexes with 4,4′-bipyrimidine and 5,5′-dicyano-2,2′-bipyridine possess uncoordinated chelating nitrogen atoms. Larger heterometallic porphyrin arrays were assembled using a combination of Sn(IV) and Rh(III) porphyrin coordination chemistry. A Sn(IV) porphyrin acted as a core around which were coordinated two isonicotinate groups, carboxylic acid functionalized porphyrins, or porphyrin trimer dendrons. Rh(III) porphyrins were coordinated to pyridyl groups at the periphery of these entities. In this way an eleven porphyrin array, with four different porphyrin metalation states, was assembled. The diamagnetic nature of both the Rh(III) and Sn(IV) porphyrins, the slow ligand exchange kinetics on the NMR time scale, and tight ligand binding permitted the porphyrin arrays to be analyzed by two-dimensional ^{1}H NMR techniques.

Introduction

The axial ligand coordination chemistry of metalloporphyrins has provided a rich field for the construction of supramolecular entities. Numerous structures ranging from discrete noncyclic arrays[1−13] to polymers,[14−25] and from cyclic oligomers[26−33] to dendrimers,[34,35] have been assembled using axial ligand coordination to metalloporphyrins. Reports of structures consisting

* To whom correspondence should be addressed. E-mail: jkms@cam.ac.uk.
† University of Cambridge.
‡ CLRC Daresbury Laboratory.

(1) Kariya, N.; Imamura, T.; Sasaki, Y. *Inorg. Chem.* **1997**, *36*, 833.
(2) Funatsu, K.; Kimura, A.; Imamura, T.; Ichimura, A.; Sasaki, Y. *Inorg. Chem.* **1997**, *36*, 1625.
(3) Giribabu, L.; Rao, T. A.; Maiya, B. G. *Inorg. Chem.* **1999**, *38*, 4971.
(4) Susumu, K.; Tanaka, K.; Shimidzu, T.; Takeuchi, Y.; Segawa, H. *J. Chem. Soc., Perkin Trans. 2* **1999**, 1521.
(5) Alessio, E.; Geremia, S.; Mestroni, S.; Srnova, I.; Slouf, M.; Gianferrara, T.; Prodi. A. *Inorg. Chem.* **1999**, *38*, 2527.
(6) Li, M.; Xu, Z.; You, X.; Huang, X.; Zheng, X.; Wang, H. *Inorg. Chim. Acta* **1997**, *261*, 211.
(7) Reek, J. N. H.; Schenning, A. P. H. J.; Bosman, A. W.; Meijer, E. W.; Crossley, M. J. *Chem. Commun.* **1998**, 11.
(8) Taylor, P. N.; Anderson, H. L. *J. Am. Chem. Soc.* **1999**, *121*, 11538.
(9) Chichak, K.; Walsh, M. C.; Branda, N. *Chem. Commun.* **2000**, 847.
(10) Darling, S. L.; Stulz, E.; Feeder, N.; Bampos, N.; Sanders, J. K. M. *New J. Chem.* **2000**, *24*, 261.
(11) Simanek, E. E.; Isaacs, L.; Li. X.; Wang, C. C. C.; Whitesides, G. M. *J. Org. Chem.* **1997**, *62*, 8994.
(12) Yamamoto, G.; Nadano, R.; Satoh, W.; Yamamoto, Y.; Akiba, K. *Chem. Commun.* **1997**, 1325.
(13) Hamstra, B. J.; Cheng, B.; Ellison, M. K.; Scheidt, W. R. *Inorg. Chem.* **2000**, *39*, 1454.
(14) Kumar, R. K.; Goldberg, I. *Angew. Chem., Int. Ed.* **1998**, *37*, 3027.
(15) Lin, K.-J. *Angew. Chem., Int. Ed.* **1999**, *38*, 2730.
(16) Michelsen, U.; Hunter, C. A. *Angew. Chem., Int. Ed.* **2000**, *39*, 764.
(17) Burrell, A. K.; Officer, D. L.; Reid, D. C. W.; Wild, K. Y. *Angew. Chem., Int. Ed.* **1998**, *37*, 114.
(18) Segawa, H.; Kunimoto, K.; Susumu, K.; Taniguchi, M.; Shimidzu, T. *J. Am. Chem. Soc.* **1994**, *116*, 11193.
(19) Sugiura, K.; Mikami, S.; Johnson, M. T.; Miller, J. S.; Iwasaki, K.; Umishita, K.; Hino, S.; Sakata, Y. *J. Mater. Chem.* **2000**, *10*, 959.
(20) Collman, J. P.; McDevitt, J. T.; Leidner, C. R.; Yee, G. T.; Torrance, J. B.; Little, W. A. *J. Am. Chem. Soc.* **1987**, *109*, 4606.
(21) Marvaud, V.; Launay, J.-P. *Inorg. Chem.* **1993**, *32*, 1376.
(22) Fleischer, E. B.; Shachter, A. M. *Inorg. Chem.* **1991**, *30*, 3763.
(23) Kobuke, Y.; Miyaji, H. *Bull. Chem. Soc. Jpn.* **1996**, *69*, 3563.
(24) Krupitsky, H.; Stein, Z.; Goldberg, I.; Strouse, C. E. *J. Inclusion Phenom. Molecular Recognition Chem.* **1994**, *18*, 177.
(25) Turner, P.; Gunter, M. J.; Hambley, T. W.; White, A. H.; Skelton, B. W. *Inorg. Chem.* **1992**, *31*, 2295.
(26) Funatsu, K.; Imamura, T.; Ichimura, A.; Sasaki, Y. *Inorg. Chem.* **1998**, *37*, 1798.
(27) Johnston, M. R.; Gunter, M. J.; Warrener, R. N. *Chem. Commun.* **1998**, 2739.
(28) Chernook, A. V.; Rempel, U.; von Borczyskowski, C.; Shulga, A. M.; Zenkevich, E. I. *Chem. Phys. Lett.* **1996**, *254*, 229.
(29) Chi, X.; Guerin, A. J.; Haycock, R. A.; Hunter, C. A.; Sarson, L. D. *J. Chem. Soc., Chem. Commun.* **1995**, 2567.
(30) Kobuke, Y.; Miyaji, H. *J. Am. Chem. Soc.* **1994**, *116*, 4111.
(31) Wojaczyński, J.; Latos-Grażyński, L. *Inorg. Chem.* **1995**, *34*, 1054.
(32) Godziela, G. M.; Tilotta, D.; Goff, H. M. *Inorg. Chem.* **1986**, *25*, 2142.
(33) Stibrany, R. T.; Vasudevan, J.; Knapp, S.; Potenza, J. A.; Emge, T.; Schugar, H. J. *J. Am. Chem. Soc.* **1996**, *118*, 3980.
(34) Mak, C. C.; Bampos, N.; Sanders, J. K. M. *Chem. Commun.* **1999**, 1085.

10.1021/ic001038f CCC: $20.00
Published on Web 03/17/2001

of multiple Rh(III) porphyrins linked by axial coordination are relatively scarce,[36−41] although Rh(III) porphyrins have received attention as receptors for amino acids/esters[42−44] and nucleobases.[45,46] We have described the preparation and crystal structure of a covalently linked Rh(III) porphyrin dimer templated by a 4,4′-bipyridine ligand and the structure of an analogous noncovalently linked complex bridged by 4,4′-bipyridine.[47] We also recently communicated the preparation of heterometallic porphyrin oligomers assembled by complementary Sn−O, Zn−N, and Ru−N coordination chemistry.[48] As it is reported that coordination of amino acids to Rh(III) porphyrins occurs through the amine moiety, and not the carboxylic acid,[45] this suggested to us that a combination of Rh(III) porphyrins and oxophilic Sn(IV) porphyrins would be suitable for construction of heterometallic architectures. In this paper we describe the synthesis and characterization of Rh(III) porphyrin complexes with multidentate nitrogen donor ligands, with a view to construction of multimetallic systems, and compare these with our previous findings. We then extend this work to encompass systems employing a Sn(IV) porphyrin carboxylate complex as a core for dendritic structures terminated at the periphery with Rh(III) porphyrins.

Experimental Section

Instrumentation. NMR spectra were recorded on Bruker DRX 500 (500.1 MHz for ^{1}H, 125.7 MHz for ^{13}C), AM 400, DRX 400 (400.1 MHz for ^{1}H, 100.6 MHz for ^{13}C), DPX 250, or AC 250 (250.1 MHz for ^{1}H, 62.9 MHz for ^{13}C) instruments. Chemical shifts are quoted in parts per million with respect to TMS. Mass spectra were recorded on Kratos MS890 (FAB, EI), Kratos Kompact MALDI IV, Bruker BioApex II (ES), Micromass Quattro (ES), and Micromass Q-TOF (ES) instruments. Infrared spectra were recorded on a Perkin-Elmer Paragon 1000 FTIR spectrometer at 4 cm^{-1} resolution or better.

X-ray Crystallography. Diffraction data were collected in Cambridge on a Rigaku R-Axis IIc or Nonius Kappa CCD device or, for small crystals, were collected at the Daresbury SRS (UK), Station 9.8, using a Bruker AXS SMART CCD area-detector.[49−51] Structures were solved with either SHELXS-97 or SIR92.[52−54] Refinement was carried out with SHELXL-97.[55] Extensive disorder was often observed in the solubilizing hexyl chains, typical of this kind of structure.[56] The carbon atoms in these disordered groups were refined with isotropic temperature factors and restrained to give chains with a reasonable geometry. Even with synchrotron radiation, crystals were found to be weakly diffracting, resulting in a relatively high R1 value.

Materials. THF, hexane, and EtOAc were distilled before use. When stated as anhydrous, solvents were distilled from an appropriate drying agent immediately prior to use. Et_3N was freshly distilled from CaH_2. Merck or Fluorochem 60 mesh silica gel was used for column chromatography. Merck silica was used for all preparations involving rhodium porphyrins.

2,7-Diazapyrene was prepared in three steps from naphthalene tetracarboxylic acid according to the literature.[57−59] 4,4′-Bipyrimidine[60] and 5,5′-dicyano-2,2′-bipyridine[61,62] were prepared using literature procedures. We have previously reported the preparation of **1**.[47] Porphyrin monomers **16**, **21**, **22**, and **23** were synthesized according to routine procedures, and details are given in the Supporting Information.

5,15-Bis(4-methoxycarbonyl-phenyl)-2,8,12,18-tetrahexyl-3,7,13,17-tetramethyl porphyrinato rhodium(III) Iodide (4). 5,15-Bis(4-methoxycarbonyl-phenyl)-2,8,12,18-tetrahexyl-3,7,13,17-tetramethyl porphyrin, prepared from 4-formyl-methylbenzoate according to a standard procedure,[63] was metalated using an analogous procedure to the synthesis of **1**.[47] The product was obtained as an orange solid (144 mg, 58%) after column chromatography on silica eluted with dichloromethane (DCM). A sample for analysis was recrystallized from DCM layered with MeOH. R_f 0.46 (DCM).

^{1}H NMR (400 MHz, $CDCl_3$): δ 10.30 (s, 2H, *meso*), 8.46 (m, 2H, Ar), 8.39 (m, 2H, Ar), 8.28 (m, 2H, Ar), 8.05 (m, 2H, Ar), 4.13 (s, 6H, OCH_3), 4.02 (m, 4H, hex H^1), 3.87 (m, 4H, hex H^1), 2.46 (s, 12H, CH_3), 2.15 (m, 8H, hex H^2), 1.74 (m, 8H, hex H^3), 1.48 (m, 8H, hex H^4), 1.39 (m, 8H, hex H^5), 0.91 (t, J = 7 Hz, 12H, hex H^6). ^{13}C NMR (100.6 MHz, $CDCl_3$): δ 167.3, 147.5, 144.8, 141.2, 140.7, 138. 4, 133.5, 133.2, 130.2, 128.8, 128.6, 119.5, 100.5, 52.4, 33.1, 31.9, 30.0, 26.9, 22.7, 15.9, 14.1. UV/vis (DCM): λ_{max} 404, 522, 550 nm. MALDI MS: m/z [M−I]$^+$ 1072. IR (CCl_4): ν_{max} 1728 (s) cm^{-1}. Anal. Calcd for $C_{64}H_{80}O_4N_4RhI\cdot CH_3OH$: C 63.41, H 6.88, N 4.55. Found: C 62.99, H 6.87, N 4.38.

(1)$_2$·DABCO (6). Prepared by titration of a solution of **1** (3.95 mg, 3.5 μmol) in $CDCl_3$ (600 μL) with DABCO in $CDCl_3$. After titration, the sample was loaded onto a silica column and eluted with hexane/DCM (1/1). The porphyrin containing eluent was evaporated, redissolved in DCM, and layered with MeOH to obtain crystals of **6** for structure determination.

^{1}H NMR (400 MHz, $CDCl_3$): δ 9.70 (s, 4H, *meso*), 7.75 (m, 8H, Ar), 7.66 (t, J = 7 Hz, 4H, Ar), 7.59 (t, J = 7 Hz, 4H, Ar), 7.37 (d, J = 7 Hz, 4H, Ar), 3.67 (m, 16H, hex H^1), 2.21 (s, 24H, CH_3), 1.82 (m, 16H, hex H^2), 1.57 (m, 16H, hex H^3), 1.43 (m, 32H, hex H^{4,5}), 0.93 (t, J = 7 Hz, 24H, hex H^6), −6.05 (s, 12H, NCH_2). ^{13}C NMR (100.6 MHz, $CDCl_3$): δ 143.9, 142.2, 139.9, 139.5, 138.1, 133.7, 132.2, 128.3,

(35) Darling, S. L.; Mak, C. C.; Bampos, N.; Feeder, N.; Teat, S. J.; Sanders, J. K. M. *New J. Chem.* **1999**, *23*, 359.
(36) Setsune, J.; Yoshida, Z.; Ogoshi, H. *J. Chem. Soc., Perkin Trans. 1* **1982**, 983.
(37) Liu, Y. H.; Anderson, J. E.; Kadish, K. M. *Inorg. Chem.* **1988**, *27*, 2320.
(38) Thomas, N. C. *Transition Metal Chem.* **1986**, *11*, 425.
(39) Kuroda, Y.; Kato, Y.; Ogoshi, H. *Chem. Commun.* **1997**, 469.
(40) Zhou, X.; Wang, R.-J.; Xue, F.; Mak, T. C. W.; Chan, K. S. *J. Organomet. Chem.* **1999**, *580*, 22.
(41) Aoyama, Y.; Yamagishi, A.; Tanaka, Y.; Toi, H.; Ogoshi, H. *J. Am. Chem. Soc.* **1987**, *109*, 4735.
(42) Aoyama, Y.; Nonaka, S.; Motomura, T.; Ogoshi, H. *Chem. Lett.* **1989**, 1877.
(43) Aoyama, Y.; Asakawa, M.; Yamagishi, A.; Toi, H.; Ogoshi, H. *J. Am. Chem. Soc.* **1990**, *112*, 3145.
(44) Aoyama, Y.; Yamagishi, A.; Asagawa, M.; Toi, H.; Ogoshi, H. *J. Am. Chem. Soc.* **1988**, *110*, 4076.
(45) Ogoshi, H.; Hatakeyama, H.; Yamamura, K.; Kuroda, Y. *Chem. Lett.* **1990**, 51.
(46) Kuroda, Y.; Hatakeyama, H.; Inakoshi, N.; Ogoshi, H. *Tetrahedron Lett.* **1993**, *34*, 8285.
(47) Kim, H.-J.; Redman, J. E.; Nakash, M.; Feeder N., Teat, S. J.; Sanders, J. K. M. *Inorg. Chem.* **1999**, *38*, 5178.
(48) Kim, H.-J.; Bampos, N.; Sanders, J. K. M. *J. Am. Chem. Soc.* **1999**, *121*, 8120.
(49) Cernik, R. J.; Clegg, W.; Catlow, C. R. A.; Bushnell-Wye, G.; Flaherty, J. V.; Greaves, G. N.; Burrows, I.; Taylor, D. J.; Teat, S. J.; Hamichi, M *J. Synchrotron Rad.* **1997**, *4*, 279.
(50) Clegg, W.; Elsegood, M. R. J.; Teat, S. J.; Redshaw, C.; Gibson, V. C. *J. Chem. Soc., Dalton Trans.* **1998**, 3037.
(51) *SMART (control) and SAINT (integration) Software*, version 4; Bruker AXS Inc.: Madison, WI, 1994.
(52) Sheldrick, G. M. *SHELXS-97. Program for the solution of crystal structures*; University of Göttingen: Germany, 1997.
(53) Burla, M. C.; Camalli, M.; Cascarano, G.; Giacovazzo, C.; Polidori, G.; Spagna, R.; Viterbo, D. *J. Appl. Crystallogr.* **1989**, *22*, 389.
(54) Altomare, A.; Cascarano, G.; Giacovazzo, C.; Guagliardi, A. *J. Appl. Crystallogr.* **1993**, *26*, 343.
(55) Sheldrick, G. M.; *SHELXL-97. Program for refinement of crystal structures*; University of Göttingen: Germany, 1997.
(56) Nakash, M.; Clyde-Watson, Z.; Feeder, N.; Teat, S. J.; Sanders, J. K. M. *Chem. Eur. J.* **2000**, *6*, 2112.
(57) Lier, E. F.; Hünig, S.; Quast, H. *Angew. Chem., Int. Ed. Engl.* **1968**, *7*, 814.
(58) Hünig, S.; Gross, J.; Lier, E. F.; Quast, H. *Liebigs Ann. Chem.* **1973**, 339.
(59) Stang, P. J.; Cao, D. H.; Saito, S.; Arif, A. M. *J. Am. Chem. Soc.* **1995**, *117*, 6273.
(60) Plé, N.; Turck, A.; Couture, K.; Quéguiner, G. *J. Org. Chem.* **1995**, *60*, 3781.
(61) Wu, H.-P.; Janiak, C.; Rheinwald, G.; Lang, H. *J. Chem. Soc., Dalton Trans.* **1999**, 183.
(62) Whittle, C. P. *J. Heterocycl. Chem.* **1977**, *14*, 191.
(63) Twyman, L. J.; Sanders, J. K. M. *Tetrahedron Lett.* **1999**, *40*, 6681.

127.7, 127.1, 119.1, 98.7, 40.0, 33.0, 31.7, 29.8, 26.6, 22.7, 15.1, 14.1. UV/vis (DCM): λ_{max} 414, 530, 558 nm.

$(1)_2$·2,7-Diazapyrene Complex (7). 2,7-Diazapyrene (2.0 mg, 9.8 μmol) and **1** (21 mg, 19 μmol) were mixed, and $CDCl_3$ (1.0 mL) was added. After stirring for 3 h, the solvent was evaporated and the residue was purified by chromatography on silica gel (hexane/DCM, 1/1 gradient to DCM) to afford the product as an orange solid (10 mg, 44%). R_f 0.30 (hexane/DCM, 1/1). Crystals for structure determination were grown from a $CHCl_3$ solution layered with hexane.

^{1}H NMR (400 MHz, $CDCl_3$): δ 10.04 (s, 4H, *meso*), 7.98 (d, J = 7 Hz, 4H, Ar), 7.65 (m, 12H, Ar), 7.52 (m, 4H, Ar), 5.64 (s, 4H, dap H^3), 3.86 (m, 8H, hex H^1), 3.71 (m, 8H, hex H^1), 2.30 (s, 24H, CH_3), 2.01 (m, 16H, hex H^2), 1.57 (m, 16H, hex H^3), 1.33 (m, 16H, hex H^4), 1.21 (m, 16H, hex H^5), 1.08 (s, 4H, dap H^2), 0.76 (t, J = 7 Hz, 24H, hex H^6). ^{13}C NMR (100.6 MHz, $CDCl_3$): δ 143.9, 142.6, 2 × 140.0, 139.7, 138.4, 133.8, 132.6, 128.2, 127.7, 127.0, 124.2, 122.0, 121.6, 119.2, 98.7, 33.1, 31.8, 29.9, 26.8, 22.6, 15.4, 14.0. UV/vis (DCM): λ_{max} 342, 420, 532, 560 nm. Anal. Calcd for $C_{134}H_{160}N_{10}Rh_2I_2$: C 67.90, H 6.80, N 5.91. Found: C 67.98, H 6.28, N 5.50.

$(1)_2$·4,4′-Bipyrimidine (8). This was prepared in an identical manner to **2**, using 4,4′-bipyrimidine instead of 4,4′-bipyridine.[47] Purification by column chromatography on silica eluting with hexane/DCM (4/3 gradient to 1/1) afforded **8** as an orange solid (33 mg, 77%). R_f 0.47 (hexane/DCM, 1/1). Crystals for structure determination were obtained from $CHCl_3$/DCM solution layered with MeOH.

^{1}H NMR (400 MHz, $CDCl_3$): δ 9.99 (s, 4H, *meso*), 7.90 (d, J = 7 Hz, 4H, Ar), 7.74 (m, 8H, Ar), 7.61 (m, 8H, Ar), 4.98 (dd, 2H, J = 6, 1 Hz, bpm H^6), 3.82 (m, 8H, hex H^1), 3.71 (m, 8H, hex H^1), 2.31 (s, 24H, CH_3), 2.00 (m, 16H, hex H^2), 1.57 (m, 16H, hex H^3), 1.37 (m, 16H, hex H^4), 1.25 (m, 16H, hex H^5), 1.07 (s, 2H, bpm H^3), 0.79 (t, J = 7 Hz, 24H, hex H^6), 0.67 (d, J = 6 Hz, 2H, bpm H^5). ^{13}C NMR (100.6 MHz, $CDCl_3$): δ 155.2, 152.7, 144.1, 142.4, 139.9, 139.6, 138.6, 133.8, 132.8, 128.3, 127.8, 127.1, 119.2, 113.9, 33.1, 31.9, 30.0, 26.9, 22.7, 15.4, 14.0. UV/vis (DCM): λ_{max} 358, 418, 530, 560 nm. Anal. Calcd for $C_{128}H_{158}N_{12}Rh_2I_2$: C 66.14, H 6.85, N 7.23. Found: C 65.94, H 6.80, N 7.08.

2,8,12,18-Tetrahexyl-3,7,13,17-tetramethyl-5,15-diphenyl-porphyrinato tin(IV) Dihydroxide (11).[64,65] $SnCl_2$ (0.10 g, 0.53 mmol) and 2,8,12,18-tetrahexyl-3,7,13,17-tetramethyl-5,15-diphenyl-porphyrin[47] (80 mg, 94 μmol) were refluxed in pyridine (5 mL) under air for 7 h and allowed to cool to room temperature. Water (20 mL) was added, and the red precipitate was filtered onto Celite and washed with MeOH (50 mL). The porphyrin was extracted from the Celite with $CHCl_3$ (70 mL), and the organic solution was washed with HCl (3 N, 2 × 20 mL) and water (2 × 20 mL), dried (Na_2SO_4), and evaporated to afford the dichloro Sn(IV) porphyrin as a red solid (95 mg, 97%).

Activity I basic alumina (10 g) was shaken with water (2 mL) until homogeneous. To this was added the dichloro Sn(IV) porphyrin (91 mg, 73 μmol) in $CHCl_3$ (10 mL). Light was excluded, and the suspension stirred for 1 d at room temperature. The suspension was filtered through Celite which was washed with $CHCl_3$ (100 mL) to remove all porphyrin. The filtrate was evaporated to afford the product as a purple solid which was used without further purification (89 mg, 100%).

^{1}H NMR (500 MHz, $CDCl_3$): δ 10.51 (s, 2H, *meso*), 8.17 (m, 4H, Ar), 7.85 (m, 2H, Ar), 7.78 (t, J = 7 Hz, 4H, Ar), 4.03 (t, J = 8 Hz, 8H, hex H^1), 2.52 (s, 12H, CH_3), 2.28 (m, 8H, hex H^2), 1.83 (m, 8H, hex H^3), 1.55 (m, 8H, hex H^4), 1.44 (m, 8H, hex H^5), 0.96 (t, J = 7 Hz, 12H, hex H^6), −7.84 (s, 2H, OH). ^{13}C NMR (100.6 MHz, $CDCl_3$): δ 2 × 144.2, 143.1, 142.3, 139.3, 133.3, 128.8, 127.9, 119.4, 97.2, 33.2, 31.9, 30.1, 29.7, 26.9, 22.8, 15.1, 14.2. UV/vis (DCM): λ_{max} 416, 548 nm. MALDI MS: m/z [M-OH]$^+$ 989. IR (CCl_4): ν_{max} 3644 (w), 2958 (s), 2930 (s), 2858 (s) cm^{-1}. Anal. Calcd for $C_{60}H_{78}N_4SnO_2$: C 71.64, H 7.81, N 5.57. Found: C 71.18, H 7.90, N 5.39.

5-(4-Carboxy-phenyl)-15-(4-pyridyl)-2,8,12,18-tetrahexyl-3,7,13,17-tetramethyl Porphyrin (17). A solution of **16** (40 mg, 44 μmol) and KOH (100 mg, 1.8 mmol) in a mixture of THF (13.5 mL) and water (125 μL) was heated to 40 °C for 1 d. Further portions of KOH (38 mg) and water (100 μL) were added, and stirring was continued at the same temperature overnight. Addition of a further portion of water (100 μL) and heating at reflux for 1 h was required to complete the reaction. After cooling to room temperature, HCl (3 N, 50 mL) was added and the solution was extracted with $CHCl_3$ (2 × 50 mL). The green organic layer was washed with water (3 × 100 mL), dried ($MgSO_4$), and evaporated to a brown solid. Column chromatography on silica eluted with DCM/EtOAc (10/1) gradient to DCM/MeOH (10/1) afforded the product as a purple solid (27 mg, 69%).

^{1}H NMR (500 MHz, CD_3OD + $CDCl_3$): δ 10.21 (s, 2H, *meso*), 8.90 (br d, 2H, pyr H^α), 8.40 (d, 2H, J = 8 Hz, Ar), 8.11 (d, 2H, J = 8 Hz, Ar), 8.07 (d, J = 5 Hz, 2H, pyr H^β), 3.91 (br, 8H, hex H^1), 2.44 (s, 6H, CH_3), 2.40 (s, 6H, CH_3), 2.12 (m, 8H, hex H^2), 1.67 (m, 8H, hex H^3), 1.41 (m, 8H, hex H^4), 1.31 (m, 8H, hex H^5), 0.84 (t, J = 7 Hz, 12H, hex H^6). ^{13}C NMR (100.6 MHz, CD_3OD + $CDCl_3$): δ 168.9, 151.5, 148.4, 147.0, 144.6, 144.1, 143.8, 143.7, 141.7, 141.4, 136.1, 135.1, 133.0, 130.5, 129.1, 128.8, 117.3, 114.0, 97.4, 2 × 33.2, 31.9, 29.9, 26.7, 22.6, 14.9, 14.7, 14.0. UV/vis (DCM): λ_{max} 408, 506, 540, 574 nm. ES MS: m/z [M + H]$^+$ calcd 900.6156, found 900.6166.

Me Ester Free-Base Dendron (24). $AsPh_3$ (26 mg, 85 μmol), $Pd_2(dba)_3$ (12 mg, 13 μmol), **23** (75 mg, 86 μmol) and **21** (50 mg, 43 μmol) were mixed and DCM (anhydrous, 3 mL) and Et_3N (anhydrous, 3 mL) added. The mixture was degassed and stirred under Ar at room temperature for 36 h. DCM (50 mL) was added to the red suspension. The solution was washed with water (3 × 30 mL), dried ($MgSO_4$) and evaporated to a red solid. After column chromatography on a short (10 cm) silica column eluted with $CHCl_3$/MeOH (50/1) and precipitation from $CHCl_3$ solution by addition of MeOH, the product was obtained as a red solid (85 mg, 75%). R_f 0.41 ($CHCl_3$/MeOH, 50/1).

^{1}H NMR (400 MHz, $CDCl_3$): δ 10.33 (s, 2H, inner *meso*), 10.26 (s, 4H, outer *meso*), 9.01 (d, J = 6 Hz, 4H, pyr H^α), 8.53 (s, 3H, Ar), 8.46 (d, J = 8 Hz, 2H, Ar), 8.21 (d, J = 8 Hz, 2H, Ar), 8.11 (d, J = 8 Hz, 4H, Ar), 8.06−8.02 (m, 8H, Ar), 4.15−3.98 (m, 27H, OCH_3, hex H^1), 2.87 (s, 6H, CH_3), 2.57 (s, 12H, CH_3), 2.51, 2.50 (2 × s, 18H, CH_3), 2.35−2.14 (m, 24H, hex H^2), 1.89−1.32 (m, 72H hex H^{3-5}), 1.00−0.88 (m, 36H, hex H^6), −2.29, −2.33, −2.40 (br s, total 6H, NH). ^{13}C NMR (100.6 MHz, $CDCl_3$): δ 167.4, 150.8, 149.0, 147.4, 145.1, 145.0, 144.6, 144.0, 143.9, 143.8, 143.7, 143.3, 142.8, 141.8, 2 × 141.7, 141.5, 136.2, 2 × 135.9, 135.3, 134.6, 133.2, 133.1, 133.0, 131.1, 130.1, 128.8, 128.5, 123.3, 123.0, 117.4, 116.9, 115.9, 114.4, 97.4, 90.8, 89.8, 52.4, 33.4, 33.3, 32.1, 2 × 32.0, 30.1, 2 × 30.0, 26.9, 26.8, 2 × 22.8, 22.7. UV/vis (DCM): 412, 508, 542, 574, 626 nm. MALDI MS: m/z [M]$^+$ 2670.

Carboxylic Acid Free-Base Dendron (25). KOH (100 mg, 1.8 mmol) and **24** (36 mg, 13 μmol) were stirred in a mixture of THF (10 mL) and water (100 μL) at 40 °C for 32 h to form a red suspension. Additional portions of KOH (25 mg, 0.45 mmol), water (200 μL), and THF (10 mL) were added, and the mixture was refluxed for 18 h under N_2. After cooling, water (30 mL) and $CHCl_3$ (50 mL) were added and HCl (3 N) added dropwise until the organic layer became green. The organic phase was separated and washed with water (3 × 30 mL), dried ($MgSO_4$), and evaporated to a red solid. Column chromatography on silica eluting with $CHCl_3$ gradient to $CHCl_3$/MeOH (20/1) followed by precipitation from $CHCl_3$ solution by addition of hexane afforded the product as a deep purple solid (15 mg, 42%). R_f 0.50 ($CHCl_3$/MeOH, 10/1).

^{1}H NMR (400 MHz, $CDCl_3$): δ 10.35 (s, 2H, inner *meso*), 10.26 (s, 4H, outer *meso*), 9.04 (d, J = 4 Hz, 4H, pyr H^α), 8.58 (d, J = 8 Hz, 2H, Ar), 8.53 (s, 3H, Ar), 8.28 (d, J = 8 Hz, 2H, Ar), 8.12−8.03 (m, 12H, Ar), 4.11, 3.99 (br m, 24H, hex H^1), 2.87 (s, 6H, CH_3), 2.57 (s, 12H, CH_3), 2.54 (s, 6H, CH_3), 2.51 (s, 12H, CH_3), 2.35−2.14 (m, 24H, hex H^2), 1.89−1.68 (m, 24H, hex H^3), 1.62 (m, 48H, hex $H^{4,5}$), 1.00−0.88 (m, 36H, hex H^6), −2.33 (br, NH). ^{13}C NMR (125.7 MHz, $CDCl_3$): δ 148.7, 145.0, 144.6, 144.0, 143.9, 2 × 143.8, 142.8, 141.7, 141.5, 136.2, 135.9, 135.2, 133.3, 133.1, 131.1, 129.3, 128.5, 123.3, 122.9, 117.4, 114.2, 97.3, 90.7, 89.7, 33.2, 2 × 32.0, 31.9, 30.1, 29.9, 26.7, 22.8, 2 × 22.7, 15.6, 15.0, 14.9, 14.1 (2 peaks). UV/vis (DCM): 412, 508, 540, 574 nm. ES MS: m/z [M]$^+$ 2657.

Me Ester Ni/Free-Base Dendron (26). This compound was prepared analogously to **24** but substituting **21** with **22**. The product was purified by silica gel chromatography eluting with DCM/EtOAc (10/1), followed

(64) Arnold, D. P. *J. Chem. Educ.* **1988**, *65*, 1111.
(65) Arnold, D. P. *Polyhedron* **1986**, *5*, 1957.

Table 1. Crystallographic Data for **1**

	1	**1**·MeOH	**1**·NCMe
empirical formula	$C_{60}H_{76}IN_4Rh$	$C_{61}H_{80}IN_4ORh$	$C_{64}H_{82}IN_6Rh$
fw	1083.06	1115.10	1165.17
cryst size, mm	0.10 × 0.08 × 0.04	0.25 × 0.15 × 0.05	0.10 × 0.06 × 0.02
space group	$P\bar{1}$	$P2_1/n$	$P2_1/n$
a, Å	12.833(4)	12.3960(10)	14.6530(10)
b, Å	14.638(5)	8.4420(10)	23.1722(17)
c, Å	14.986(5)	25.574(2)	34.574(3)
α, deg	91.099(5)	90	90
β, deg	107.205(5)	93.540(10)	96.673(5)
γ, deg	97.343(6)	90	90
V, Å^3	2662.2(15)	2671.1(4)	11659.8(14)
Z	2	2	8
ρ_{calc}, Mg/m^3	1.351	1.386	1.328
R	0.1290	0.0660	0.1219
wR2	0.3187	0.1698	0.2761
goodness of fit on F^2	1.111	1.147	1.075

by a second column eluted with $CHCl_3$/MeOH (50/1). The product was obtained as a red solid (99 mg, 89%). R_f 0.34 ($CHCl_3$/MeOH, 50/1).

^{1}H NMR (400 MHz, $CDCl_3$): δ 10.27 (s, 4H, outer *meso*), 9.51 (s, 2H, inner *meso*), 8.98 (d, J = 6 Hz, 4H, pyr H$^\alpha$), 8.44 (d, J = 2 Hz, 1H, Ar), 8.36 (d, J = 8 Hz, 2H, Ar), 8.31 (d, J = 2 Hz, 2H, Ar), 8.08 (d, J = 8 Hz, 4H, Ar), 8.01 (m, 10H, Ar), 4.11 (s, 3H, OCH_3), 3.99 (m, 16H, hex H^1), 3.77 (t, J = 7 Hz, 4H, hex H^1), 3.66 (t, J = 8 Hz, 4H, hex H^1), 2.62 (s, 6H, CH_3), 2.56 (s, 12H, CH_3), 2.49 (s, 12H, CH_3), 2.24−2.01 (m, 30H, CH_3, hex H^2), 1.79−1.34 (m, 72H, hex H$^{3-5}$), 1.02−0.90 (m, 36H, hex H^6), −2.39 (s, 4H, NH). ^{13}C NMR (125.7 MHz, $CDCl_3$): δ 167.3, 150.7, 149.0, 146.4, 145.0, 144.5, 144.4, 143.9, 143.7, 142.8, 142.3, 141.7, 141.5, 140.4, 139.9, 2 × 139.7, 138.5, 136.2, 135.9, 135.2, 134.5, 133.2, 133.0, 131.0, 129.9, 128.6, 128.4, 123.1, 122.9, 117.4, 115.4, 114.6, 114.3, 97.3, 96.7, 90.7, 89.7, 52.3, 33.3, 33.0, 32.8, 2 × 31.9, 2 × 29.9, 29.8, 26.8, 26.4, 26.3, 22.8, 22.7, 16.2, 15.5, 14.9, 14.2, 14.1. UV/vis (DCM): 412, 508, 570 nm. MALDI MS: *m*/*z* [M]$^+$ 2727.

Carboxylic Acid Ni/Free-Base Dendron (27). Compound **27** was prepared similarly to **25**. After chromatography on a silica column eluted with toluene/MeOH (100/1 gradient to 10/1), the product was obtained as a red solid (38 mg, 90%). R_f 0.15 (toluene/MeOH, 10/1).

^{1}H NMR (400 MHz, $CDCl_3$): δ 10.27 (s, 4H, outer *meso*), 9.54 (s, 2H, inner *meso*), 9.04 (d, J = 4 Hz, 4H, pyr H$^\alpha$), 8.43 (m, 3H, Ar), 8.30 (d, J = 1 Hz, 2H, Ar), 8.11−8.00 (m, 14H, Ar), 3.99 (br, 16H, outer hex H^1), 3.79 (br, 4H, inner hex H^1), 3.70 (br, 4H, inner hex H^1), 2.61 (s, 6H, inner CH_3), 2.57 (s, 12H, outer CH_3), 2.51 (s, 12H, outer CH_3), 2.29 (s, 6H, inner CH_3), 2.19 (m, 16H, outer hex H^2), 2.07 (m, 8H, inner hex H^2), 1.78−1.63 (m, 24H, hex H^3), 1.57−1.33 (m, 48H, hex H^{4,5}), 0.99 (t, J = 7 Hz, 6H, inner hex H^6), 0.95 (t, J = 7 Hz, 6H, inner hex H^6), 0.91 (t, J = 7 Hz, 24H, outer hex H^6), −2.3 (br, NH). ^{13}C NMR (100.6 MHz, $CDCl_3$): δ 170.3, 151.4, 148.4, 146.6, 145.0, 144.6, 144.4, 144.0, 143.9, 143.7, 142.7, 142.5, 141.8, 141.5, 140.4, 140.0, 139.7, 138.6, 138.5, 136.2, 135.9, 135.2, 133.4, 133.0, 131.1, 129.2, 128.6, 123.2, 123.0, 117.5, 115.6, 114.6, 114.1, 97.4, 96.8, 90.8, 89.7, 33.4, 33.1, 32.9, 2 × 32.0, 30.0, 29.9, 29.7, 29.4, 26.8, 26.4, 22.9, 2 × 22.8, 16.3, 15.6, 15.0, 14.9, 14.3, 2 × 14.2. UV/vis (DCM): 412, 508, 570, 626 nm. MALDI MS: *m*/*z* [M]$^+$ 2712.

Results and Discussion

Rh(III) Porphyrin Building Block. The Rh(III) porphyrin, **1**, was prepared and purified according to a previously described procedure.[47,66] Recrystallization of **1** from chloroform or dichloromethane layered with methanol afforded almost black crystals which were formulated as a methanol solvate. The ^{1}H NMR spectrum of this material when dissolved in $CDCl_3$ typically displayed a broadened quartet, integrating to one proton, in the range of −2 to −2.4 ppm. This was assigned to the hydroxyl proton of an axially coordinated methanol molecule which was introduced during the recrystallization step. The methanol CH_3 resonance was usually obscured by the more intense hexyl methylene resonances at 1.36−2.22 ppm. This solvent remains coordinated to the porphyrin in the solid state, even after months of storage and extensive drying in vacuo. In further support of our assignment of the resonances of coordinated methanol was the observation that addition of dried molecular sieves to the NMR sample resulted in an upfield shift of the hydroxyl resonance to −2.48 ppm and appearance of the CH_3 resonance at 1.02 ppm. After standing over the sieves overnight, both resonances vanished as the methanol was absorbed by the sieves. Titration of methanol into a solution of **1**·MeOH in $CDCl_3$ resulted in downfield shifts of both the OH and CH_3 resonances, indicating that exchange of free and bound methanol is fast on the NMR chemical shift time scale. A peak initially at 1.17 ppm was also observed to shift downfield during this titration, and this was assigned to water which competes with methanol for coordination to the rhodium center.

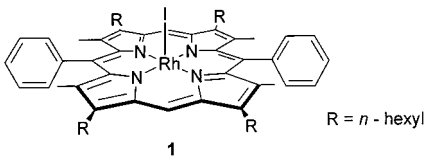

1

A THF solvate of **1** could be obtained by dissolution of freshly purified **1** in THF, followed by evaporation of the solvent and drying in vacuo. The ^{1}H NMR spectrum of this material in $CDCl_3$ displayed an eight proton broadened peak with a shoulder at 0.42 ppm which can be assigned to the overlapping resonances of weakly coordinated THF. As the **1**·MeOH or **1**·THF solvates possess a well defined composition, but a labile axial ligand, they were used as the starting materials for the self-assembly experiments described in this paper.

Crystals of **1**·MeOH suitable for X-ray diffraction were obtained from a dichloromethane/methanol solvent mixture. The structure is shown in Figure 1 and confirms the presence of a single methanol molecule coordinated to the Rh center in the solid state. The Rh atom lies on an inversion center, and the axial iodo and alcohol ligands are disordered. The porphyrin itself shows little deviation from planarity, with an rms deviation of 0.03 Å from the best fit plane.

In an attempt to organize dimeric porphyrin architectures in the solid state utilizing coordination of rhodium porphyrins to diols, **1** was crystallized from solvent mixtures containing ethylene glycol or propylene glycol. After several months, a two phase mixture of a dichloromethane solution of **1** and ethylene glycol afforded crystals which were found not to

(66) Wayland, B. B.; Ba, S.; Sherry, A. E. *J. Am. Chem. Soc.* **1991**, *113*, 5305.

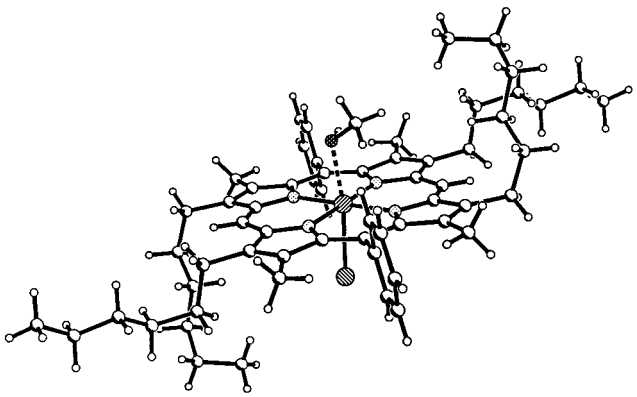

Figure 1. Molecular structure of **1**·MeOH.

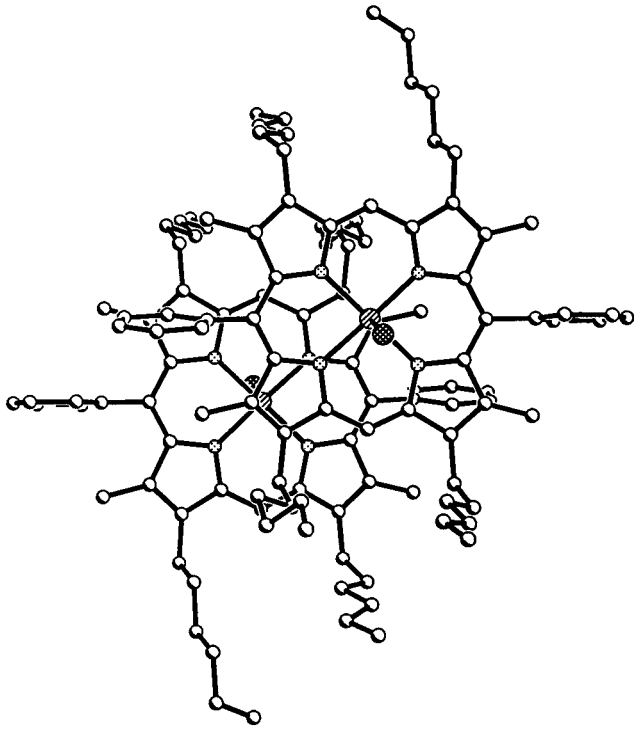

Figure 2. Molecular structure of unsolvated **1**.

contain a coordinated diol but tightly π stacked dimers in which the rhodium is only five coordinate (Figure 2). The absence of a sixth ligand permits the porphyrins to approach to a separation of only 3.2 Å in the offset geometry predicted for $\pi-\pi$ stacking. Evidently there is a balance between weak coordination of an alcohol ligand and π stacking in the solid state, an effect which we have also observed for Zn porphyrins.[56]

Rh(III) Complexes with Bridging Ligands. In our previous work[47] we reported the preparation, ^{1}H NMR spectrum, and crystal structure of the complex of **1** with 4,4′-bipyridine, **2**. During the course of that work we were surprised to isolate **2** as the product of the reaction of **1** with excess 4,4′-bipyridine, which led us to suspect that the 1:1 complex **3** was formed initially and that this was converted to **2** during the isolation procedure. A ^{1}H NMR titration of **1**·MeOH in $CDCl_3$ solution with 4,4′-bipyridine revealed that this is indeed the case. On addition of up to 0.5 equiv of 4,4′-bipyridine, the only product observed was **2** and displaced methanol, which appeared as a doublet at the expected chemical shift of 3.49 ppm. No uncoordinated pyridyl groups could be observed. Further addition of 4,4′-bipyridine resulted in the appearance of a new set of resonances attributed to **3** and uncoordinated 4,4′-bipyridine. The chemical shifts and complexation induced shifts ($\Delta\delta$) of this species are given in Figure 3. The complexation induced shifts of **2** are almost exactly the sum of the two sets observed in **3**, implying additivity of the ring current effects. The cooperativity coefficient,[67] defined as $\alpha = K/4$, where K is the equilibrium constant for the reaction of Equation 1, can be calculated from the integrations of the resonances of each species. For this system we determined $\alpha = 1.9$ indicating that the porphyrins bind largely independently to each end of the ligand. The value of α expected for truly independent binding is 1.0 on statistical grounds; larger numbers correspond to anticooperative behavior.

$$P_2L + L \overset{K}{\rightleftharpoons} 2PL \quad (P = \text{porphyrin, L} = \text{bidentate ligand}) \quad (1)$$

Although all species were in slow exchange on the NMR time scale, the possibility of isolation of mixed porphyrin complexes of the type P^1-bipyridine$-P^2$ is precluded by exchange of the porphyrin units on a practical time scale. Addition of **4** to a $CDCl_3$ solution of **2** afforded a mixture of all of the possible dimeric and monomeric porphyrin complexes as evidenced by the observation of six β-methyl resonances in the ^{1}H NMR spectrum.

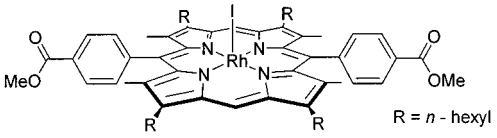

4

A solution containing largely **3** and excess 4,4′-bipyridine was passed through a silica column eluted with hexane/dichloromethane (1/1). The eluent was found to contain exclusively **2** because the polar 4,4′-bipyridine is retained on the column thus shifting the equilibrium of eq 1 toward the left. The comparatively nonpolar **2** readily elutes from the silica gel. Similarly, recrystallization of a solution of **3** and excess 4,4′-bipyridine from $CHCl_3$ layered with methanol afforded crystals containing an enhanced proportion of **2** as the 4,4′-bipyridine is readily soluble in methanol.

We also examined the coordination of DABCO to **1** and observed similarities to the behavior of 4,4′-bipyridine. An ^{1}H NMR titration of **1**·MeOH with DABCO in $CDCl_3$ enabled the chemical shifts of the complexes **5** and **6** to be determined (Figure 4). All species were in slow exchange on the chemical shift time scale at room temperature. In this case the $\Delta\delta$ values are not precisely additive, and we measure $\alpha = 85$ (average of two determinations) thus implying moderately anticooperative binding. It is clear from the X-ray structure of **6** (Figure 5) that the porphyrin substituents can come into contact with each other, which restricts their conformational freedom and could contribute toward the anticooperative binding of the porphyrin units. We previously described a similar inhibition of a second binding of a Ru(II) porphyrin to DABCO.[34] Passage of a solution of **5** and excess DABCO through silica gel eluted with hexane/dichloromethane (1/1) retained excess DABCO on the silica and effected the conversion of **5** to **6**.

For comparison with 4,4′-bipyridine, we prepared 2,7-diazapyrene according to the literature.[57−59] This ligand is slightly larger than 4,4′-bipyridine, and constrained to planarity. Reaction of **1** with 2,7-diazapyrene afforded complex **7**. The ^{1}H NMR complexation induced shift of H^α (Figure 6) is indeed

(67) Connors, K. A.; Pendergast, D. D. *J. Am. Chem. Soc.* **1984**, *106*, 7607.

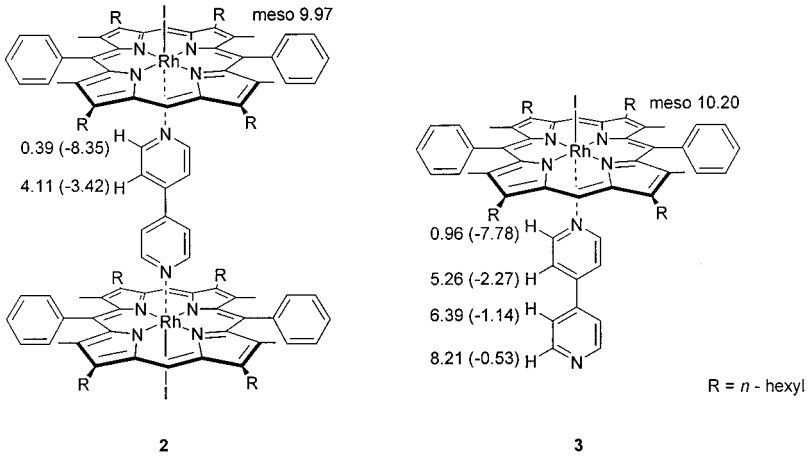

Figure 3. Chemical shifts (ppm) and complexation induced shifts in parentheses of **2** (ref 47) and **3**.

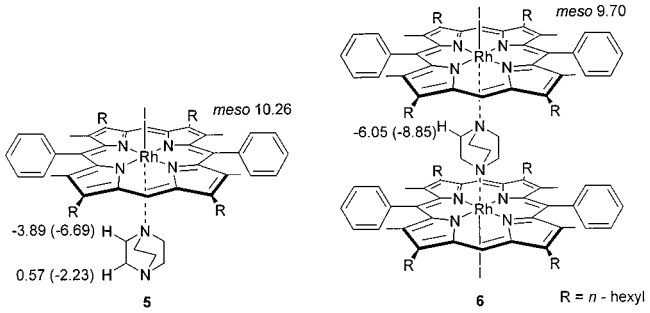

Figure 4. Chemical shifts (ppm) and complexation induced shifts in parentheses of **5** and **6**.

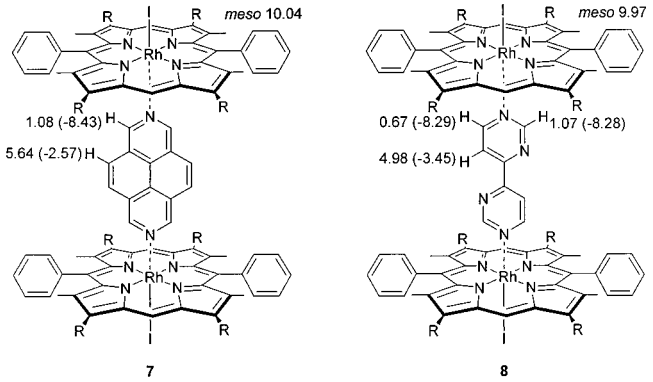

Figure 6. Chemical shifts (ppm) and complexation induced shifts in parentheses of **7** and **8**.

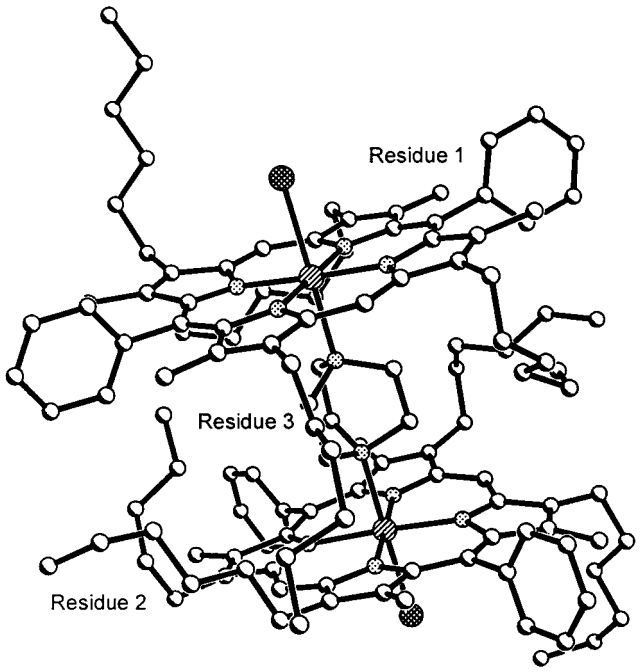

Figure 5. Molecular structure of **6**.

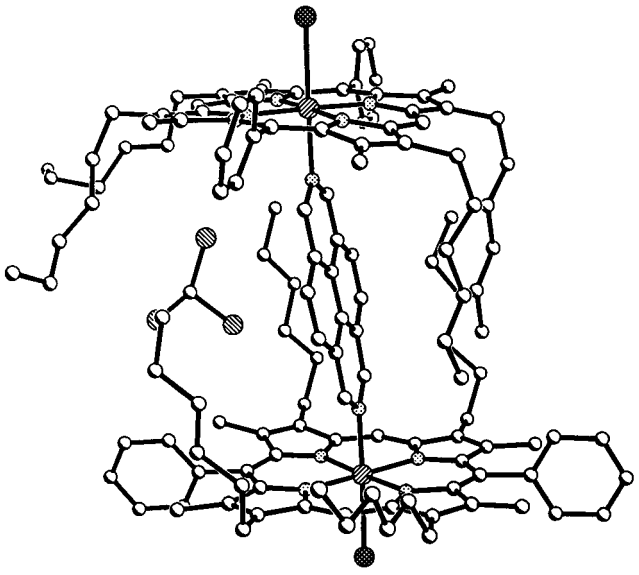

Figure 7. Molecular structure of **7**.

very similar to its value in **2**, confirming that the complexes have similar geometries in solution. However, the X-ray structure of **7** differs considerably from that of **2** in that in the former the porphyrin units are rotated at 83° with respect to each other (Figure 7), whereas in the latter the aryl axes of the porphyrins are parallel. The molecules pack in such a way that the hexyl chains are folded around the diazapyrene group and a chloroform solvent molecule. The tilting of the ligand from the perpendicular to the porphyrin is less extreme than that observed in the structure of **2**, with angles of 79.24(3)° and 76.04(4)° between the diazapyrene and porphyrin best fit planes. The α protons are oriented between the pyrrole nitrogen atoms in the conformation proposed to give rise to minimum steric clash.[68] The Rh−N bond lengths of 2.115(4) Å and 2.091(4) Å are almost identical to those observed for **2** (2.121(4) Å).

We chose to investigate multidentate ligands with both bridging and chelating coordination modes as these could

(68) Collins, D. M.; Countryman, R.; Hoard, J. L. *J. Am. Chem. Soc.* **1972**, *94*, 2066.

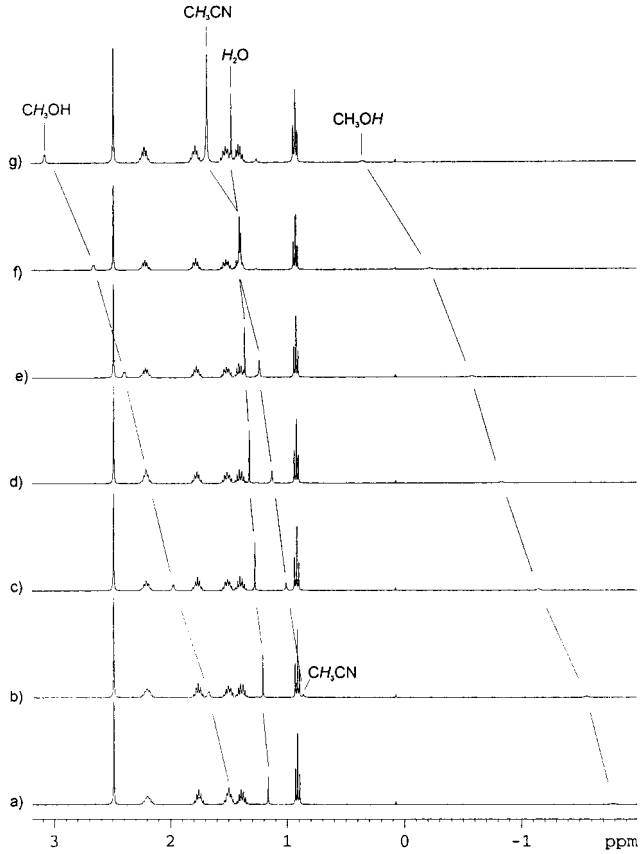

Figure 8. A 400 MHz ^{1}H titration of **1**·MeOH with MeCN in $CDCl_3$: (a) 0 equiv; (b) 0.2 equiv; (c) 0.6 equiv; (d) 1.0 equiv; (e) 1.8 equiv; (f) 3.0 equiv; (g) 5.4 equiv.

potentially bridge between porphyrins while simultaneously coordinating a third metal at the chelating site. Porphyrin coordination at the chelating site is prevented on steric grounds. The ligand 4,4′-bipyrimidine was attractive in this respect as it presents divergent nitrogen donors resembling those of 4,4′-bipyridine, while offering the diversity of coordination chemistry available to 2,2′-bipyridine. Reaction of an excess of 4,4′-bipyrimidine with **1**, followed by chromatography, afforded complex **8** presumably via initial formation of a 1:1 complex. The ^{1}H NMR complexation induced shifts of **8** are given in Figure 6 and are practically identical to those of **2**, attesting to the close geometric similarity between the two complexes. Crystals of **8** were grown under identical conditions to those used for the crystallization of **2**. X-ray structure determination revealed **8** to be almost isostructural to **2**, except for the additional two nitrogen atoms of the 4,4′-bipyrimidine ligand which are disordered over two sites. The ligand, which is "buried" between the porphyrins, appears to have made no difference to the conformation and packing of the molecules in the crystal.

As an alternative to aromatic nitrogen heterocycles, we investigated the coordination of nitriles to **1**. An ^{1}H NMR titration of **1**·MeOH in $CDCl_3$ with MeCN revealed a progressive downfield shift of both the MeOH and MeCN resonances and a further singlet assigned to water (Figure 8). All species were in fast exchange between free and porphyrin-bound forms on the chemical shift time scale at room temperature. After addition of 5 equiv of MeCN, the chemical shift of the methanol CH_3 resonance still had not reached that expected for methanol in $CDCl_3$, indicating that methanol competes effectively for coordination to the porphyrin. This result suggested that coordinating solvents must be avoided if nitrile coordination to

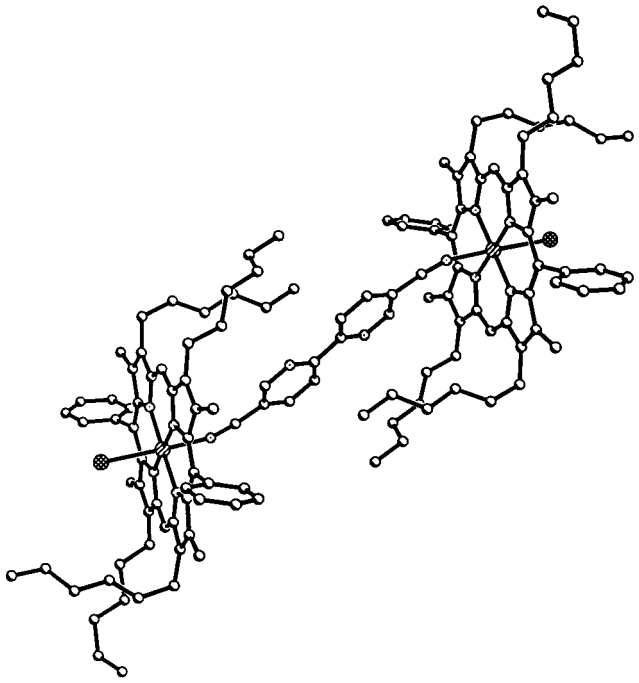

Figure 9. Molecular structure of **9**.

1 is to be a successful means of organizing the porphyrins. With this in mind, a solution of **1**·MeOH in dichloromethane was filtered through silica gel, in an attempt to remove methanol, before addition of 0.4 equiv 5,5′-dicyano-2,2′-bipyridine. Addition of cyclohexane resulted in slow formation of crystals which X-ray analysis revealed to be the complex **9** (Figure 9) in which a pair of Rh(III) porphyrins are bridged by the cyano groups of the ligand. The axis of the bipyridyl group is severely

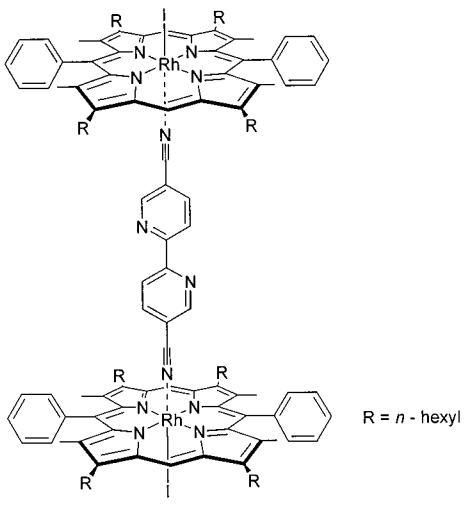

9

tilted with respect to the normal of the porphyrins, which gives rise to a reduced separation between the planes of the porphyrin groups and a lateral offset. The "pivot point" is predominantly the nitrile N atom and the bond angle Rh(1)−N(5)−C(61) is 155.9(2)°, although the nitrile group itself is slightly bent with an N(5)−C(61)−C(62) angle of 171.8(3)°. We propose that the potential energy function for bending of Rh−N−C from 180° has a gentle slope permitting tilting of the ligand from an in vacuo energy minimum at perpendicularity to allow for optimal packing in the solid state. A packing plot (Figure 10) shows that the molecules of **9** are interdigitated with each other and

Table 2. Crystallographic Data for **6**, **7**, **8**, and **9**

	6	**7**	**8**	**9**
empirical formula	$C_{127}H_{166}Cl_2I_2N_{10}Rh_2$	$C_{134.50}H_{160.50}Cl_{1.50}I_2N_{10}Rh_2$	$C_{130}H_{162}Cl_4I_2N_{12}Rh_2$	$C_{144}H_{182}I_2N_{12}Rh_2$
fw	2363.22	2430.02	2494.14	2540.64
crystals size, mm	0.16 × 0.08 × 0.02	0.14 × 0.14 × 0.10	0.14 × 0.08 × 0.04	0.06 × 0.06 × 0.02
space group	$P2_1/c$	Cc	$P\bar{1}$	$P\bar{1}$
a, Å	14.8653(8)	15.0183(2)	12.2300(10)	14.4222(10)
b, Å	34.7225(18)	29.6207(5)	15.2190(10)	14.6677(10)
c, Å	23.6103(12)	29.2941(5)	17.2930(10)	16.5079(11)
α, deg	90	90	96.060(10)	93.492(2)
β, deg	108.140(2)	102.350(5)	110.390(10)	110.978(2)
γ, deg	90	90	90.530(10)	93.249(2)
V, Å^3	11581.0(10)	12730.0(3)	2996.5(4)	3243.0(4)
Z	4	4	1	1
ρ_{calc}, Mg/m^3	1.355	1.268	1.382	1.301
R	0.1373	0.0440	0.0738	0.0420
wR2	0.2755	0.1146	0.2056	0.0978
goodness of fit on F^2	1.214	1.053	1.565	1.017

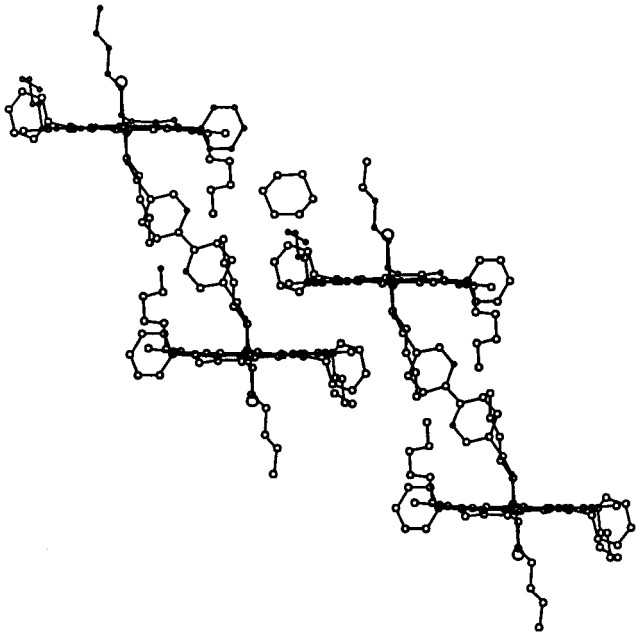

Figure 10. Packing of **9** in the solid state.

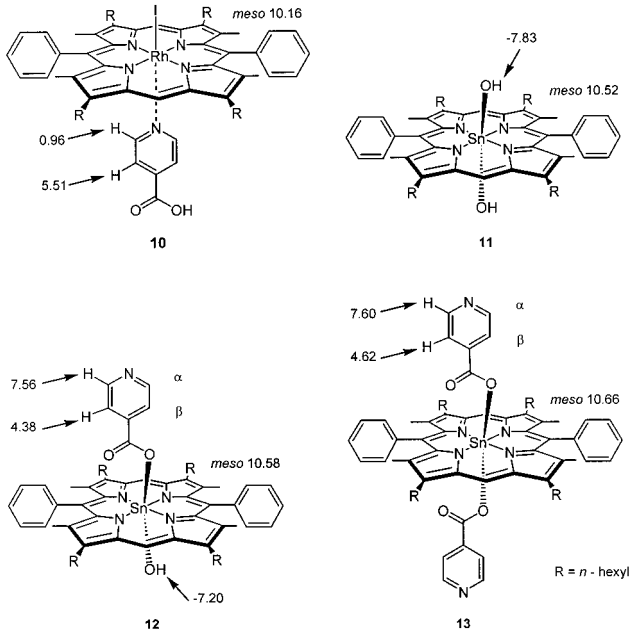

Figure 11. Selected chemical shifts (ppm) of **10**−**13**.

that remaining space is occupied by a cyclohexane molecule. A tilted geometry is certainly not a general feature of the coordination of nitriles to **1**. The structure of an MeCN solvate of **1** features two crystallographically inequivalent porphyrins with coordinated MeCN molecules which are almost perpendicular to the plane of the porphyrin with Rh−N−C angles of 176.8(13)° and 177.0(15)°. The bipyridyl unit of **9** lies on an inversion center so that the N−C−C−N torsion angle is 180° by symmetry and the aryl rings are coplanar. This conformation permits conjugation of the aryl groups while avoiding steric clash between the 3 and 3′ hydrogen atoms. In the structure of **9** the Rh−N_{axial} bond length of 2.054(2) Å is shorter than the corresponding lengths in the structures of **2**, **7**, and **8**. Short bonds to the axial ligands of 2.075(14) Å and 2.062(14) Å were also observed in the structure of **1**·MeCN, although due to the poor quality of the data this result is of less significance than in **9**. The difference in bond lengths between the nitriles and aromatic heterocycles may arise from differences in the donor orbital, the former possessing a greater degree of *s* character leading to poorer donor ability but a shorter bond. A steric effect could also be involved as the nitriles lack the H^{α} protons which make a close approach to the porphyrin plane in **2**, **7**, and **8**.

Self-Assembly Using Complementary Rh(III) and Sn(IV) Coordination Chemistry. As discussed in the Introduction, the combination of Sn(IV) and Rh(III) porphyrins appeared attractive for the construction of large heterometallic entities using porphyrin coordination chemistry. As an initial control experiment to verify that carboxylic acids do not bind to **1** or cause other adverse effects such as protonation, a solution of **1**·MeOH in $CDCl_3$ was titrated with benzoic acid. Small (∼0.1 ppm) chemical shift changes of the benzoic acid aryl protons were observed during this titration, although no significant changes in the porphyrinic resonances were observed. These results may be explained by weak coordination of the benzoic acid to the porphyrin or may simply arise due to concentration dependence of the carboxylic acid chemical shifts.

Isonicotinic acid was chosen as the simplest ligand possessing both a pyridyl group and a carboxylic acid for coordination to Rh(III) and Sn(IV), respectively. The 1,4 disposition of these functionalities was selected to avoid a steric clash between simultaneously bound porphyrins. The portionwise addition of a suspension of isonicotinic acid to a solution of **1** in $CDCl_3$ was monitored by ^{1}H NMR spectroscopy. This afforded the 1:1 complex **10**, in which the isonicotinic acid is bound through the nitrogen atom. The chemical shifts of this species are given in Figure 11. Crystallization of this compound from a non-hydrogen bonding solvent was expected to afford a hydrogen bonded carboxylic acid dimer.[69] However, crystals obtained

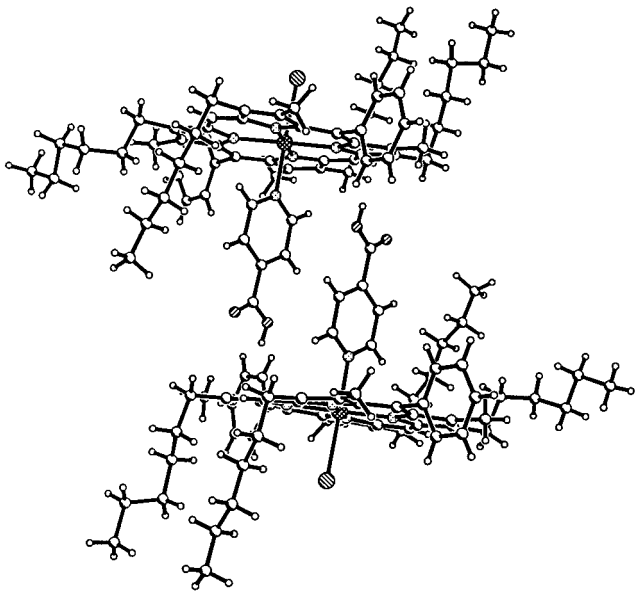

Figure 12. Crystal structure of **10**.

from a dichloromethane/hexane mixture did not display this hydrogen bonding motif, but instead consisted of a collapsed structure (Figure 12) in which a pair of isonicotinic acid moieties lie parallel and offset to each other with the acidic proton directed toward a pyrrole ring of an adjacent porphyrin. The carboxylic acid proton is not disordered over the two oxygen atoms, as evidenced by the C−O bond lengths of 1.315(8) and 1.202(7) Å consistent with a single and a double bond. The porphyrin is almost exactly planar with an rms deviation of 0.07 Å from the least squares best fit plane. The driving force which favors this structure in preference to a hydrogen bonded dimer may be the requirement of dense packing in the crystal. In the structures of **2**, **8**, and **9** this requirement is met by tilting and inclusion of solvent, whereas in **10** efficient packing is achieved by foregoing hydrogen bonds and adoption of the observed slipped structure.

The reaction of Sn(IV) porphyrin **11** in $CDCl_3$ with isonicotinic acid was monitored by ^{1}H NMR spectroscopy (Figure 13). The hydroxyl resonance of **11** was observed as a singlet at −7.83 ppm with satellites due to coupling to $I = {}^1/_2$ isotopes of Sn. Addition of isonicotinic acid suspension resulted in a broadening of the hydroxyl resonance, and formation of the 1:1 complex **12** within minutes, with concomitant sharpening of the hydroxyl resonance. On standing overnight at room temperature **12** equilibrated to a mixture of **11**, **12**, and **13** (Figure 13c). The kinetic preference for formation of a 1:1 Sn(IV) carboxylate complex, followed by equilibration has been observed previously.[70] Addition of further portions of isonicotinic acid, allowing time for equilibration to occur, yielded a solution in which **13** was the predominant species. Selected chemical shifts of **12** and **13** are given in Figure 11.

Addition of 0.9 eq **1**·THF to this solution resulted in an increase in the complexity of the ^{1}H NMR spectrum due to the presence of the three porphyrinic species **13**, **14**, and **15** and THF displaced from **1**. A COSY spectrum was acquired to correlate the α and β resonances of the isonicotinate groups of each of these species. The chemical shifts are given in Figure 14. Further addition of **1** simplified the spectrum, which could be interpreted in terms of a mixture of **15** and excess **1** (Figure 13f). From this sample, crystals of **15** suitable for structure determination were obtained. The structure is shown in Figure 15. The Sn atom lies on an inversion center, so that the two Rh

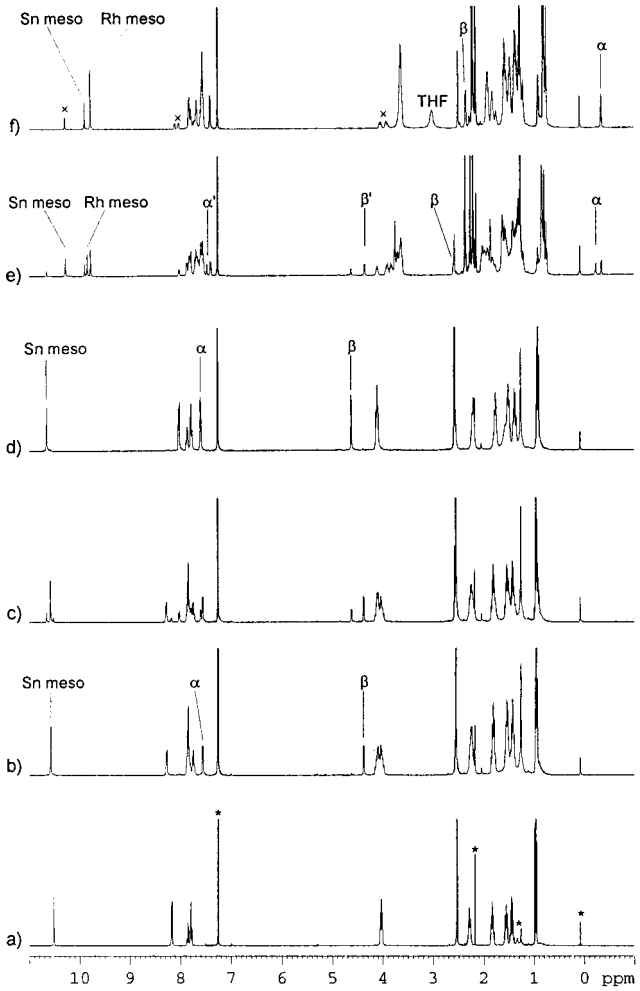

Figure 13. A 400 MHz ^{1}H NMR titration of **11** in $CDCl_3$ with isonicotinic acid followed by **1**·THF: (a) **1**, solvent/impurity peaks are marked by *; (b) **12**; (c) after equilibrating overnight; (d) **13**; (e) **13** + <2 equiv of **1**, peaks of **14** are labeled; (f) **15**, × marks peaks due to excess **1**.

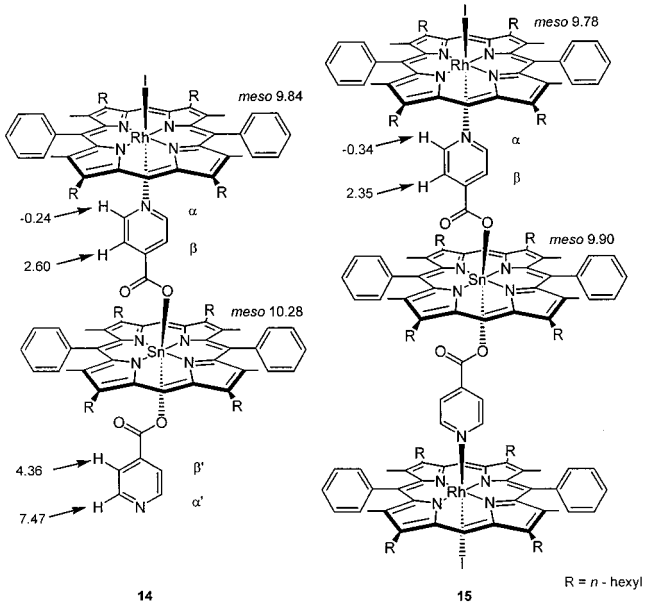

Figure 14. Selected chemical shifts of **14** and **15**.

(69) Leiserowitz, L. *Acta Crystallogr.* **1976**, *B32*, 775.
(70) Hawley, J. C.; Bampos, N.; Abraham, R. J.; Sanders, J. K. M. *Chem. Commun.* **1998**, 661.

porphyrins are equivalent by symmetry. The Rh porphyrins are almost exactly planar with an rms deviation from the best fit plane of 0.06 Å. The whole isonicotinate moiety is also planar and perpendicular to the Rh porphyrin, with an angle between the best fit planes of 89.97(6)°. The Sn porphyrin unit is slightly tilted with respect to the Rh porphyrins with an angle between the best fit planes of 8.64(5)°. In the solid, the molecules are interdigitated such that the volume between the stack of porphyrins is filled by neighboring molecules (Figure 16).

This self-assembly strategy was extended to prepare arrays of porphyrins by replacing the isonicotinic acid with a porphyrin-based building block. Porphyrin **17** was prepared via methyl ester **16**. As **17** was found to be largely insoluble in $CDCl_3$,

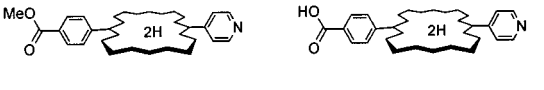

16 **17**

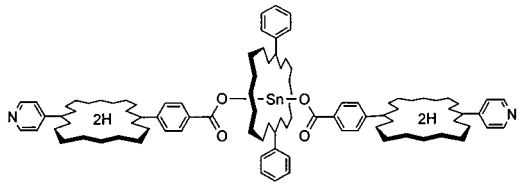

18

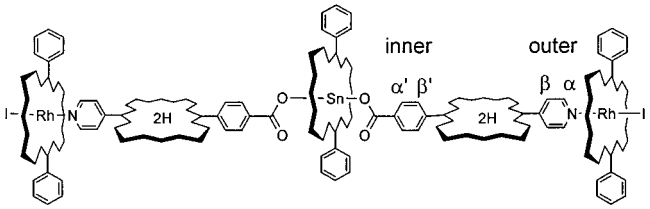

19

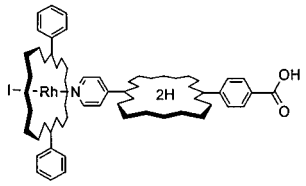

20

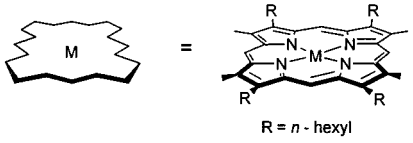

weighed amounts of **11** and **17** in a 1:2 molar ratio were mixed in $CDCl_3$. Dissolution was assisted by sonication and gentle warming. After 2 d, an ^1H NMR spectrum was acquired and a pair of characteristic doublets at 7.03 and 5.19 ppm were assigned to the bound aryl carboxylate of **18**. The major peaks in the downfield region of the spectrum can be assigned to the *meso* resonances of the Sn and free-base porphyrin units of **18** (Figure 17). Addition of 2 equiv **1**·THF afforded **19** as the major species. In the ^1H NMR spectrum the free-base porphyrin pyridyl H^{β} resonance is clearly visible at 5.70 ppm, and the H^{α} resonance was identified at 1.17 ppm from a COSY spectrum.

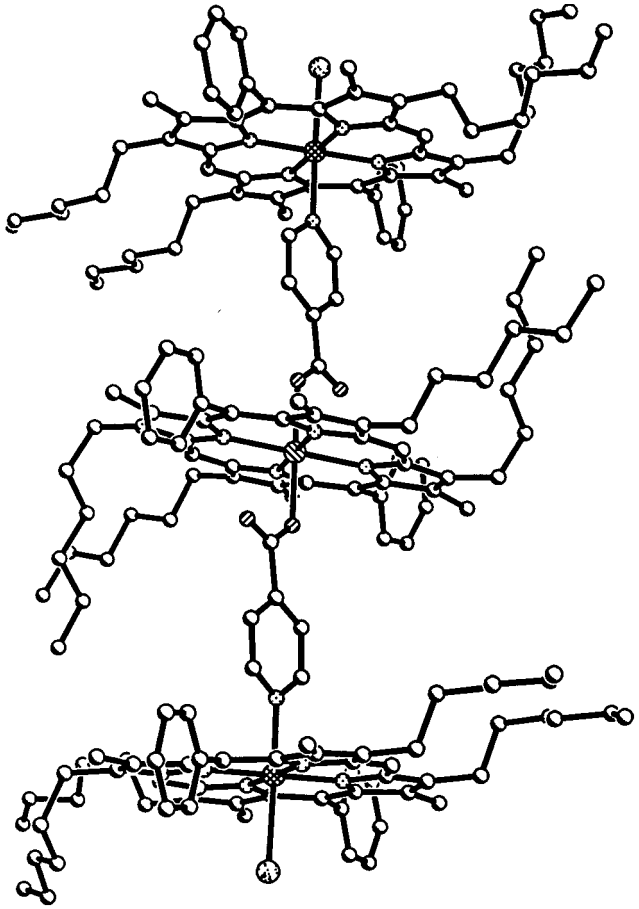

Figure 15. Molecular structure of **15**.

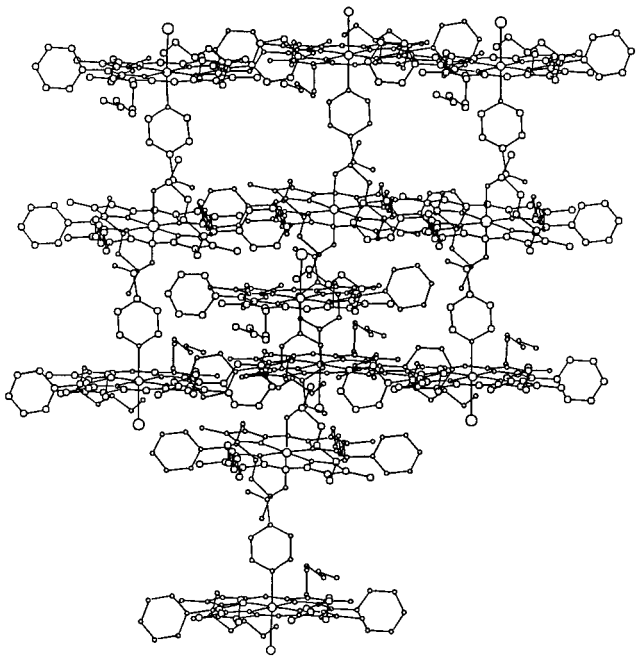

Figure 16. Packing of **15** in the solid state.

An NOE links the H^{β} peak to the outer β-methyl at 0.72 ppm. The aryl carboxylate appears as a pair of doublets at 6.86 ($H^{\beta'}$) and 5.08 ppm ($H^{\alpha'}$), and these show an NOE to the inner β-methyl at 1.64 ppm.

The Sn porphyrin *meso* resonance was identified at 10.80 ppm by integration. The free-base porphyrin lies within the shielding region of both the Sn and Rh porphyrins, and

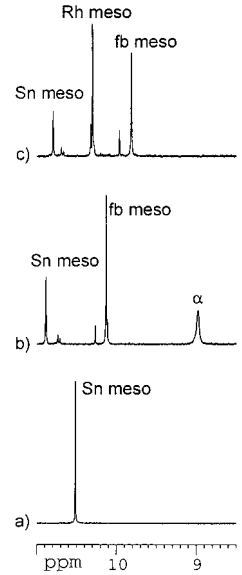

Figure 17. Assembly of **19** in $CDCl_3$. Downfield region of the 400 MHz ^{1}H NMR spectra, with assignments of the major peaks. Minor peaks are due to an unidentified impurity: (a) **11**; (b) **18**; (c) **19**.

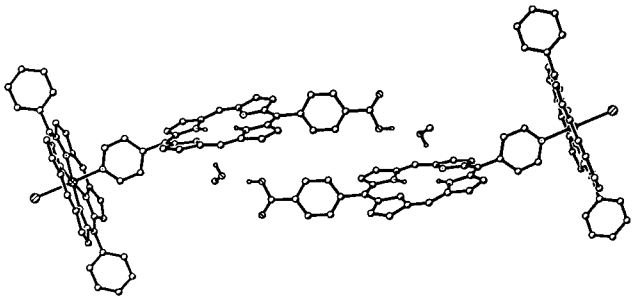

Figure 18. Crystal structure of **20** showing hydrogen bonding to methanol molecules. Porphyrin alkyl substituents have been omitted for clarity.

consequently the *meso* resonance appears upfield shifted at 9.81 ppm. This assignment is also consistent with the NOE connectivity, with cross-peaks connecting the resonances in the sequence: *meso* → hexyl H^1 → β-methyl → aryl. The free-base porphyrin has two degenerate tautomers in which the pyrrolic protons are inequivalent. Exchange of these protons is slow on the chemical shift time scale, resulting in a pair of broadened resonances at −3.08 and −3.27 ppm.

Although crystallization from a methanol containing solvent mixture was successful for **15**, when this technique was applied to **19** the crystals obtained were found to be composed of **20**. The Sn porphyrin unit has dissociated, most likely due to slow displacement of the carboxylate by the excess methanol present in the solvent. The structure of **20** (Figure 18) displays a hydrogen bond network between the acid group, a methanol molecule and the porphyrin pyrrolic nitrogen atom which organizes the molecules of **20** into dimeric units in the solid. Such hydrogen bonding of alcohols to the core of free-base porphyrins has been encountered previously.[71−73] The ^{1}H NMR spectrum of the crystals not used for structure determination was consistent with the composition of **20**, confirming that the crystal selected for diffraction was representative of the bulk.

Table 3. Crystallographic Data for **10**, **15**, and **20**

	10	**15**	**20**
empirical formula	$C_{66}H_{81}IN_5O_2Rh$	$C_{192}H_{236}I_2N_{14}O_4Rh_2Sn$	$C_{121}H_{154}IN_9O_3Rh$
fw	1206.17	3382.26	2012.34
cryst size, mm	0.16 × 0.13 × 0.12	0.18 × 0.06 × 0.01	0.16 × 0.06 × 0.06
space group	$P\bar{1}$	$P\bar{1}$	$P\bar{1}$
a, Å	12.3970(4)	16.6542(5)	11.9139(5)
b, Å	14.8480(3)	17.7629(6)	16.7586(7)
c, Å	17.2500(6)	17.8328(6)	28.6361(11)
α, deg	94.7580(18)	117.1100(10)	104.2840(10)
β, deg	109.8380(13)	94.2950(10)	98.3090(10)
γ, deg	90.4860(18)	109.7730(10)	91.6610(10)
V, Å^3	2974.22(15)	4250.5(2)	5470.1(4)
Z	2	1	2
ρ_{calc}, Mg/m^3	1.347	1.321	1.222
R	0.0397	0.0591	0.0467
wR2	0.0984	0.1788	0.1249
goodness of fit on F^2	1.075	1.083	1.029

Further extension of the self-assembly strategy was based on our previous work on coordination arrays of Ru porphyrins.[35] We designed a porphyrin trimer dendron **24**, which was prepared using Pd catalyzed coupling[74] according to Scheme 1. Hydrolysis of the methyl ester protecting group afforded the dendron **25** which presents a convergent carboxylic acid for coordination to a Sn(IV) porphyrin core and divergent pyridyl groups for coordination to Rh(III) porphyrins. The synthesis permits introduction of a metalated porphyrin at either or both the inner or outer positions of the dendron, by metalation prior to the coupling step. In this way the mixed nickel and free-base porphyrin dendron **27** was prepared.

The assembly of porphyrin arrays was carried out as a two stage titration, thus enabling observation, by ^{1}H NMR spectroscopy, of the intermediates in the assembly process. Compound **11** was mixed with 3 equiv of dendron **25** in $CDCl_3$, and the ^{1}H NMR spectrum was recorded 35 min after mixing. This spectrum (Figure 19a) shows peaks assigned to the complex **28**, unreacted **25**, and an intermediate, postulated to be a 1:1 complex. After 2 h, the intensity of peaks due to the intermediate

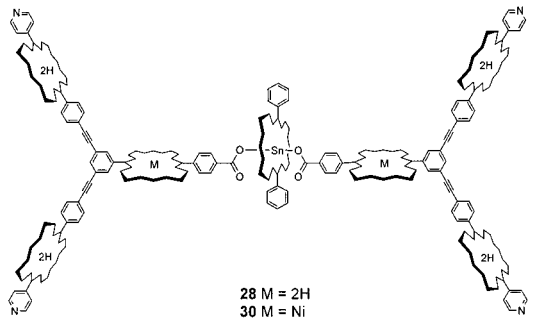

had diminished. Aliquots of **11** were titrated in over 2 d, until the predominant species was **28** (Figure 19b). The resonances of the bound aryl carboxylate of the inner porphyrin appear clearly as a pair of doublets at 7.09 and 5.22 ppm. Into the solution of **28** was titrated **1**·MeOH. Addition of <4 equiv of **1** yielded complex ^{1}H NMR spectra with many *meso* resonances which we are unable to assign (Figure 19c). This arises from the presence of six species in which zero to four of the pyridyl groups of **28** are coordinated to **1**. As **1** was added, the intensity of the pyridyl H$^\alpha$ resonance at ∼9.0 ppm decreased and a new

(71) Senge, M. O.; Medforth, C. J.; Forsyth, T. P.; Lee, D. A.; Olmstead, M. M.; Jentzen, W.; Pandey, R. K.; Shelnutt, J. A.; Smith, K. M. *Inorg. Chem.* **1997**, *36*, 1149.
(72) Einstein, F. W. B.; Jones, T. *Acta Crystallogr.* **1984**, *C40*, 696.
(73) Balaban, T. S.; Eichhöfer, A.; Lehn, J.-M. *Eur. J. Org. Chem.* **2000**, 4047.
(74) Wagner, R. W.; Johnson, T. E.; Li, F.; Lindsey, J. S. *J. Org. Chem.* **1995**, *60*, 5266.

Scheme 1[a]

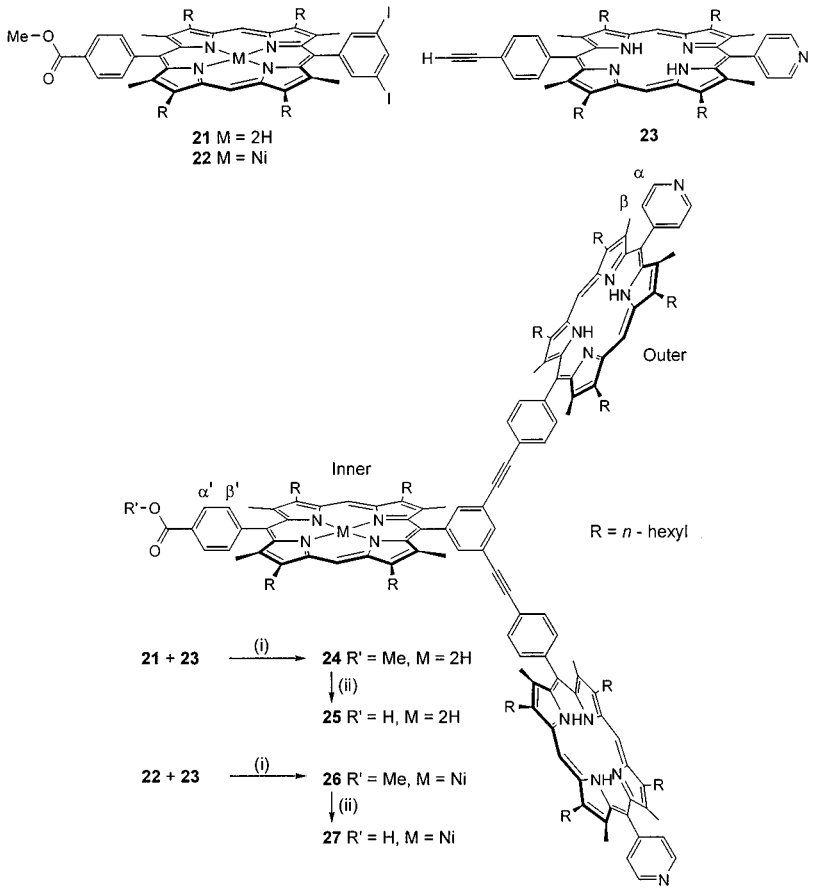

[a] Reagents and conditions: (i) $Pd_2(dba)_3$, $AsPh_3$, Et_3N, DCM, rt; (ii) KOH, THF, H_2O, reflux, then HCl.

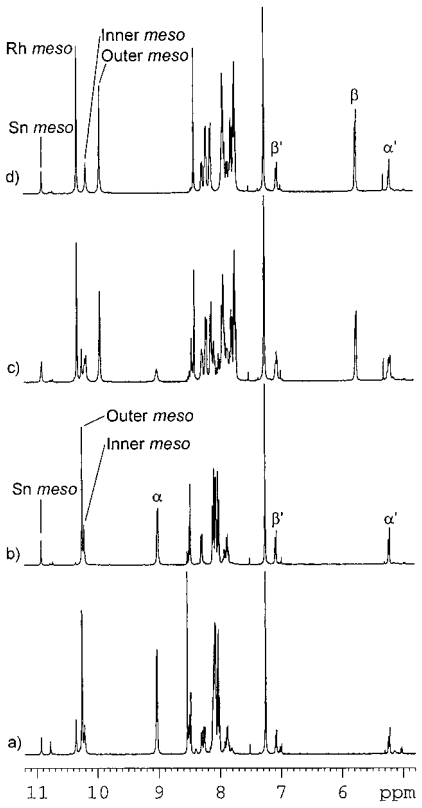

Figure 19. Assembly of **29** in $CDCl_3$. Downfield region of the 400 MHz ^1H NMR spectra: (a) **11** + 3 equiv of **25**, 35 min after mixing; (b) **28**; (c) **28** + 3 equiv of **1**·MeOH; (d) **29**.

doublet appeared at 5.75 ppm assigned to H^{β} of pyridyl groups coordinated to **1**. After addition of 4 equiv of **1**, the spectrum (Figure 19d) simplified considerably due to the absence of species with unbound pyridyl groups, leaving **29** as the major species in solution. COSY and NOESY spectra were acquired to assist in the assignment of the resonances of **29**. The NOE

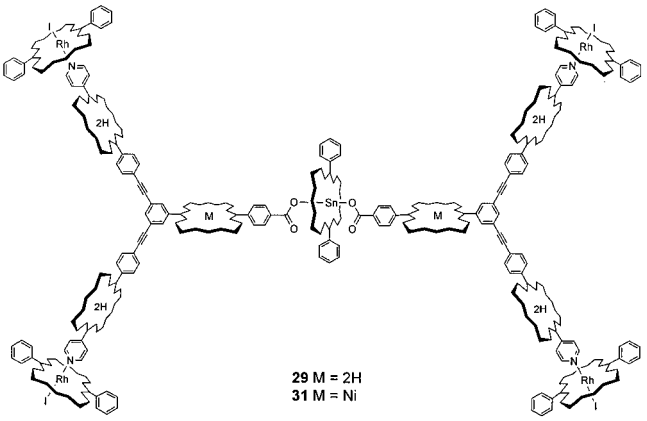

connectivity of **29** is depicted in Figure 20. NOEs to the pyridyl and aryl carboxylate protons enable the β-methyl and hexyl groups of the inner and outer free-base porphyrins to be assigned. The inner(inner) and outer(outer) β-methyls of the dendron are closest to the Sn and Rh porphyrins and as a consequence are shielded and were located among the hexyl resonances at 1.81 and 0.79 ppm, respectively. Additional support for the proposed structure comes from the observation of a weak NOE between the outer(outer) β-methyl group and

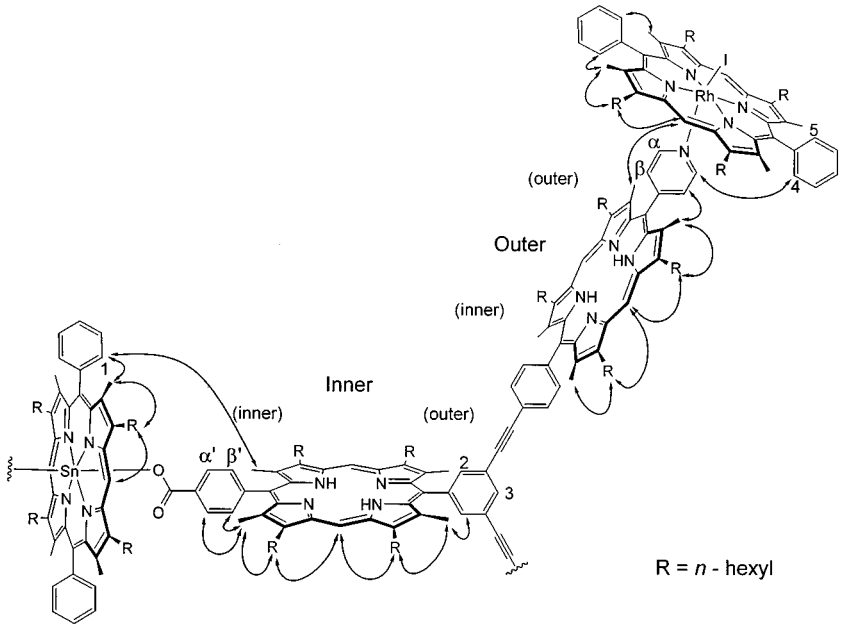

Figure 20. NOE connectivity of **29**. An NOE is represented by a double headed arrow. Labeling for ^{1}H NMR assignments is shown.

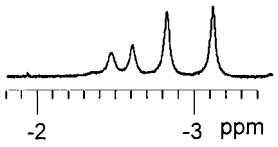

Figure 21. Upfield region of the 400 MHz ^{1}H NMR spectrum of **29**.

the Rh porphyrin *meso* protons, confirming the close spatial proximity of the two porphyrins enforced by Rh−pyridyl coordination. Another weak NOE is observed between a doublet at 8.28 ppm, assigned to the Sn porphyrin aryl group, and the inner(inner) β-methyl. The pyridyl H$^\alpha$ resonance was located at 1.21 ppm from its cross-peak to H$^\beta$ in the COSY spectrum. Although the hexyl resonances overlap extensively, the hexyl H^1 resonances can be unambiguously assigned from the NOESY spectrum, and the remaining resonances of each hexyl spin system located using the TOCSY technique. As was observed with **19**, the exchange of the pyrrolic protons is slow on the chemical shift time scale and this results in two NH resonances for each of the inner and outer free-base porphyrins (Figure 21).

The assembly of the array **31** was carried out analogously, via **30**, which was titrated with **1**·MeOH (Figure 22). The ^{1}H NMR spectrum of **31** was assigned using 2D techniques as previously discussed for **29**. The nickel porphyrin, which only weakly coordinates axial ligands, does not interfere with the assembly of the array. The *meso* resonance of the Ni porphyrin unit of **31** occurs upfield of the free-base, Rh and Sn *meso* resonances. This is an intrinsic feature of the Ni porphyrin, with the *meso* resonance of **22** appearing at 9.46 ppm, whereas that of free-base **21** occurs at 10.25 ppm. The shielded resonances of the pyridyl groups occur as doublets at 1.21 and 5.76 ppm, and the aryl carboxylate at 5.04 and 6.82 ppm.

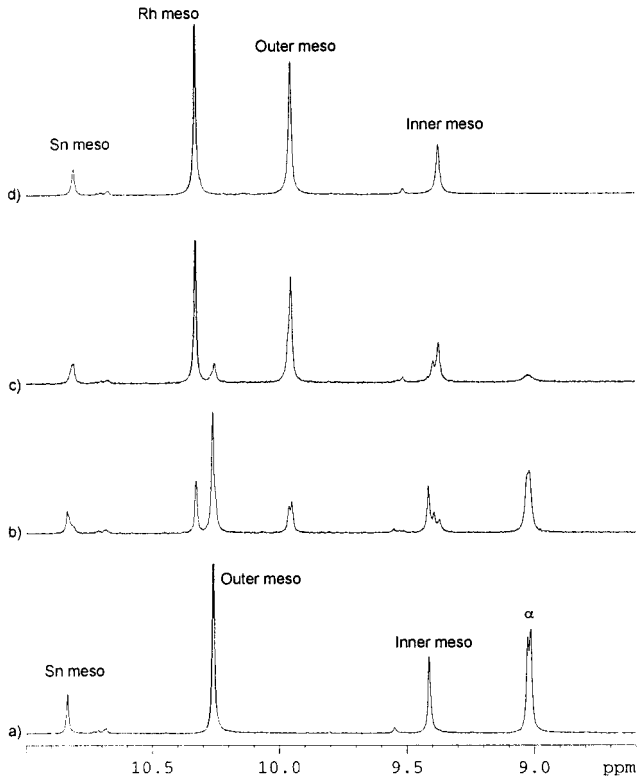

Figure 22. Assembly of **31** in $CDCl_3$. Downfield region of the 400 MHz ^{1}H NMR spectra: (a) **30**; (b) **30** + 1 equiv of **1**; (c) **30** + 3 equiv of **1**; (d) **31**.

Conclusions

In summary, we have demonstrated the assembly of structures containing multiple Rh(III) porphyrins using axial coordination to multidentate nitrogen donor ligands. With the bidentate ligands DABCO, 4,4′-bipyridine, and 4,4′-bipyrimidine, the distribution of products could be altered to favor a dimeric structure by silica gel column chromatography or recrystallization which would serve to remove excess ligand. Complexes of Rh(III) porphyrin with 4,4′-bipyrimidine and 5,5′-dicyano-2,2′-bipyridine both leave the chelating nitrogen atoms free, with the potential to coordinate an additional metal ion. In the solid-state structures of these complexes, a tilted geometry of the ligand with respect to the porphyrin plane can be ascribed to a crystal packing effect. Larger heterometallic porphyrin arrays could be constructed using a combination of Sn(IV) and Rh(III) porphyrin coordination chemistry. A Sn(IV) porphyrin acted as a core unit around which was coordinated two isonicotinate groups, carboxylic acid functionalized porphyrins, or porphyrin

trimer dendrons. Rh(III) porphyrins were coordinated to pyridyl groups at the periphery of these entities. The diamagnetic nature of both porphyrins, slow ligand exchange kinetics on the NMR time scale, and tight ligand binding facilitated the analysis of these species by multidimensional ^{1}H NMR techniques.

Acknowledgment. We thank EPSRC and Avecia for financial support. We thank Dr. N. Bampos, Dr. Y. -F. Ng, A. Mason, and D. Howe for assistance with NMR measurements. Dr. E. Stulz and G. Kaiser are thanked for MALDI mass spectra.

Supporting Information Available: Details of the preparation and spectroscopic data of **16**, **21**, **22**, and **23**; enlargements of Figures 8, 13, and 19; full ^{1}H NMR spectra of **19**, **29**, and **31**; and crystallographic data of **1**, **1**·MeOH, **1**·NCMe, **6**, **7**, **8**, **9**, **10**, **15**, and **20** in CIF format; equations of least squares planes and deviations from them. This material is available free of charge via the Internet at http://pubs.acs.org.

IC001038F